Available online at www.sciencedirect.com
ScienceDirect
Journal of the European Ceramic Society 31 (2011) 733–738
www.elsevier.com/locate/jeurceramsoc

Structural, thermal and mechanical properties of transparent Yb:$(Y_{0.97}Zr_{0.03})_2O_3$ ceramic

Xiaorui Hou [a,b], Shengming Zhou [a,*], Tingting Jia [a,b], Hui Lin [a], Hao Teng [a]

[a] *Key Laboratory of Material Science and Technology for High Power Lasers, Shanghai Institute of Optics and Fine Mechanics, Chinese Academy of Sciences, P.O. Box 800-211, Shanghai 201800, China*
[b] *Graduate School of Chinese Academy of Sciences, Beijing 100049, China*

Received 3 August 2010; received in revised form 22 November 2010; accepted 30 November 2010
Available online 23 December 2010

Abstract

Yb doped $(Y_{0.97}Zr_{0.03})_2O_3$ transparent ceramics were fabricated by solid state reaction and vacuum sintering. The microstructure, thermal and mechanical properties of Y_2O_3 ceramic, as well as the effect of Yb doping concentration on these properties were investigated in detail. The lattice parameter and unit cell volume decrease with the increasing of Yb content, whereas thermal expansive coefficient increases. With Yb content increasing from 0 to 8 at.%, the mean grain size increases from 15.82 μm to 26.54 μm, and the thermal conductivity at room temperature (RT) decreases from 11.97 to 6.39 W/m/K. The microhardness decreases with Yb content, and the microhardness and fracture toughness of $(Y_{0.97}Zr_{0.03})_2O_3$ transparent ceramic is 11.11 GPa and 1.29 MPa $m^{1/2}$, respectively.

Keywords: Y_2O_3; Transparent ceramics; Mechanical properties; Thermal properties; Sintering

1. Introduction

One of the most important achievements in modern laser material science is the development of transparent ceramics based on the cubic oxides $Y_3Al_5O_{12}$ and RE_2O_3 (RE = Y, Sc, Lu or Gd), doped with trivalent lanthanides (Ln^{3+}). Among them, Y_2O_3 transparent ceramic has received great attention due to its high thermal conductivity (~13.5 W/K m), good chemical stability, broad range of transparency (0.2–8 μm), relatively low phonon energy (~430–550 cm^{-1}) and the capacity of doping with rare earth (RE^{3+}) ions.[1,2]

Yb^{3+} ions, with the simplest energy level construction, have some important advantages: (1) low quantum defects (8.6%) between the pump and the laser photons, which results in low heat generation during lasing[3]; (2) long storage lifetime of the upper laser level (1.3 ms); (3) no excited state absorption or upconversion loss.[4,5] Most importantly, its intense and broad absorption band near 940 nm makes it highly suitable for InGaAs diode pumping. Recent years, diode-pumped high power CW laser,[6] passively Q-switched laser,[7] passively mode-locked and femtosecond laser have been reported with polycrystalline Yb:Y_2O_3 ceramic,[8] and the highest slope efficient of CW laser in Yb:Y_2O_3 ceramic has reached 82.4%.[9]

As we all know, during laser operation, the laser induced damage and laser beam quality are much related with the physical properties of the host materials. The light absorption of laser material causes thermal gradient which may disturb the laser oscillation and directly affect the quality of laser beam and laser efficiency.[10] Moreover, the thermal gradients can also lead to material fracture if they are high enough. The mechanical properties of laser material are very important for the equipment design and practical use. So besides the optical properties, the structural, mechanical and thermal properties are all important parameters to assess a laser material. The thermal conductivity of Lu_2O_3 and LuAG ceramics has been reported by Peters et al.,[11,12] and the thermal and mechanical properties of YAG transparent ceramic were investigated in detail.[13,14] But a sys-

* Corresponding author. Tel.: +86 21 69918482; fax: +86 21 69918607.
E-mail addresses: xrhou1983@163.com (X. Hou), zhousm@siom.ac.cn (S. Zhou).

0955-2219/$ – see front matter © 2010 Elsevier Ltd. All rights reserved.
doi:10.1016/j.jeurceramsoc.2010.11.038

Table 1
Cell parameters of Yb doped Y_2O_3 transparent ceramics.

Yb concentration (at.%)	Lattice parameter (nm)	Unit cell volume (nm^3)
0	1.05947 ± 0.00023	1.18921 ± 0.00078
3	1.05846 ± 0.00004	1.18585 ± 0.00013
5	1.05751 ± 0.00006	1.18263 ± 0.00021
8	1.05714 ± 0.00013	1.18142 ± 0.00045

tematic investigation of thermal and mechanical properties of Yb doped Y_2O_3 transparent ceramic is less known to the best of our knowledge. Our previous work investigated the effect of ZrO_2 on Y_2O_3 ceramic sintering and the spectroscopic properties of Yb:$(Y_{0.97}Zr_{0.03})_2O_3$ transparent ceramic.[15,16] In this work, Yb doped $(Y_{0.97}Zr_{0.03})_2O_3$ ceramics with 2 in. in diameter were fabricated to investigate the structural, thermal (thermal diffusivity, conductivity and expansion) and mechanical properties (microhardness and fracture toughness), as well as the effect of Yb doping content on these properties.

2. Experimental

High purity (99.999%) Y_2O_3 and Yb_2O_3 were used as starting materials with 3.0 at.% ZrO_2 as additive. According to the formula $(Y_{0.97-x}Zr_{0.03}Yb_x)_2O_3$ ($x = 0$ (S1), 0.03 (S2), 0.05 (S3) and 0.08 (S4)), the powders were blended and ball milled in absolute ethyl alcohol for 24 h with agate balls. After dried, disks with 2 in. in diameter were compacted in steel mold at 30 MPa and then isostatically pressed at 250 MPa. Transparent ceramics were obtained after sintered at 1800 °C under a base pressure of $\sim 1.0 \times 10^{-3}$ Pa for 20 h.

The specimens were polished on both sides to measure the optical transmittance with JASCO V-900 UV/VIS/NIR spectrophotometer (JASCO, Japan). The structure of ceramics was determined by X-ray diffraction (XRD, Cu target, Model Ultima IV, Rigaku, Japan). JSM 6360-LA scanning electron microscopy (SEM) was used to analyze the microstructure of ceramics. The samples (5 mm × mm 5 × 50 mm) for thermal-expansion measurement were cut from the as-grown transparent ceramics and measured on dilatometry DIL 402PC (NETZSCH German). Thermal diffusion coefficient and specific heat of the transparent ceramic were measured by the laser flash method using a laser flash apparatus (NETZSCH LFA 447 Nanoflash). The samples (10 mm × 10 mm × 2 mm) were double-side polished and coated with graphite to carry out the measurements. The Vickers microhardness and fracture toughness of Yb doped Y_2O_3 transparent ceramic (20 mm × 20 mm × 2 mm) were obtained from 20 indentations made by Digital Vickers Hardness Tester FV-700 (Future-Tech, Japan). In this study, the maximum load is 1 kg and the dwell time is 15 s, and the length of indentation diagonals and radical cracks was measured from the SEM images.

3. Results and discussion

3.1. Densification and microstructure

All the sintered samples present high transparency and the average total transmittance of 2 mm thick sample is 75.67%. As shown in Fig. 1(a), the samples demonstrate high transmittance not only in near infrared but also in visible region, which indicates that the ceramics have high quality without scattering centers. The integrated X-ray diffraction profiles of $(Y_{0.97}Zr_{0.03})_2O_3$ transparent ceramics with different Yb doping concentrations are presented in Fig. 1(b). We can see that the phase structure of the ceramics is almost the same despite of the different Yb contents. All the samples are well crystallized and coincided well with cubic Y_2O_3 phase (JCPDS 41-1105). While inspecting carefully, it can be observed that all the diffraction peaks show a slight movement to higher diffraction angles, which is a clear evidence of the shrinkage of the unit cell. We calculate the lattice parameter and unit cell volume based on the XRD patterns, which are shown in Table 1, both of them decrease with the increasing of Yb content. It is mainly due to the smaller radius of Yb^{3+} ($R = 0.86$ Å) and Zr^{4+} ion ($R = 0.80$ Å) compared with that of Y^{3+} ion ($R = 0.90$ Å).

The microstructure of the polished surface was investigated after etched in H_3PO_4 for 3 min at 85 °C. As shown in Fig. 2, the grain size of all samples is comparatively homogeneous without abnormal grain growth regardless of Yb content, and the grain boundaries are clear without any pores or impurities. It is easily observed that the grain size increases with Yb concentration. We measured the mean grain size by averaging over 300 grains using a mean linear intercept method. The mean grain size increases from 15.82 μm to 18.91 μm, 22.14 μm and 26.54 μm when the concentration

Table 2
Microhardness and fracture toughness of Y_2O_3 ceramics with different Yb doping contents.

Sample	Average indentation diagonal, d (μm)	Average length of radial cracks, C (μm)	Microhardness, H (GPa)	Fracture toughness, K_{IC} ($MPa\,m^{1/2}$)
Pure Y_2O_3	40.43	61.98	11.11 ± 0.28	1.29 ± 0.05
3 at.% Yb:Y_2O_3	40.75	69.22	10.94 ± 0.17	1.1 ± 0.05
5 at.% Yb:Y_2O_3	41.31	70.94	10.64 ± 0.12	1.07 ± 0.04
8 at.% Yb:Y_2O_3	43.51	71.79	9.59 ± 0.21	1.12 ± 0.06
Ref. 19			~10	~2.5
Ref. 20			7.23 ± 0.35 9.09 ± 0.41	0.81 ± 0.07 1.39 ± 0.07

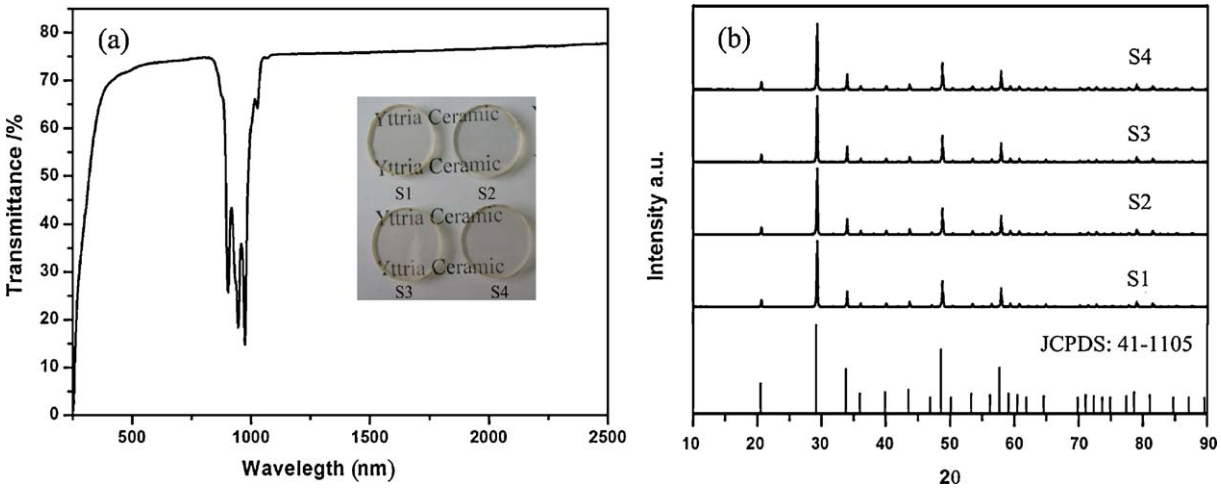

Fig. 1. (a) Transmittance curve of 5 at.% Yb doped $(Y_{0.97}Zr_{0.03})_2O_3$ transparent ceramic. Inset: photographs of $(Yb_xY_{0.97-x}Zr_{0.03})_2O_3$ transparent ceramics. (b) XRD patterns of $(Y_{0.97}Zr_{0.03})_2O_3$ transparent ceramics with different Yb doping concentrations.

of Yb^{3+} ion is 0, 3.0 at.%, 5.0 at.% and 8.0 at.%, respectively. The reason can be explained as below: the radius difference between Yb^{3+} and Y^{3+} ion will induce lattice distortion, which would enhance the mass transport at grain boundaries during sintering. And this distortion will become larger with the content of Yb^{3+} ion increasing, so the speed of mass transport and grain growth increases accordingly and the grains grow larger.

3.2. Thermal properties

Before the thermal expansion measurement, the samples were heated at 500 °C for 10 h with an extremely slow heating and cooling rate of 20 °C/h. The main purpose of the annealing is to relieve the processing stress. The experimental data we got was the thermal expansion length (dL/L_0) with the increasing of temperature, as shown in Fig. 3(a). We can see that the ther-

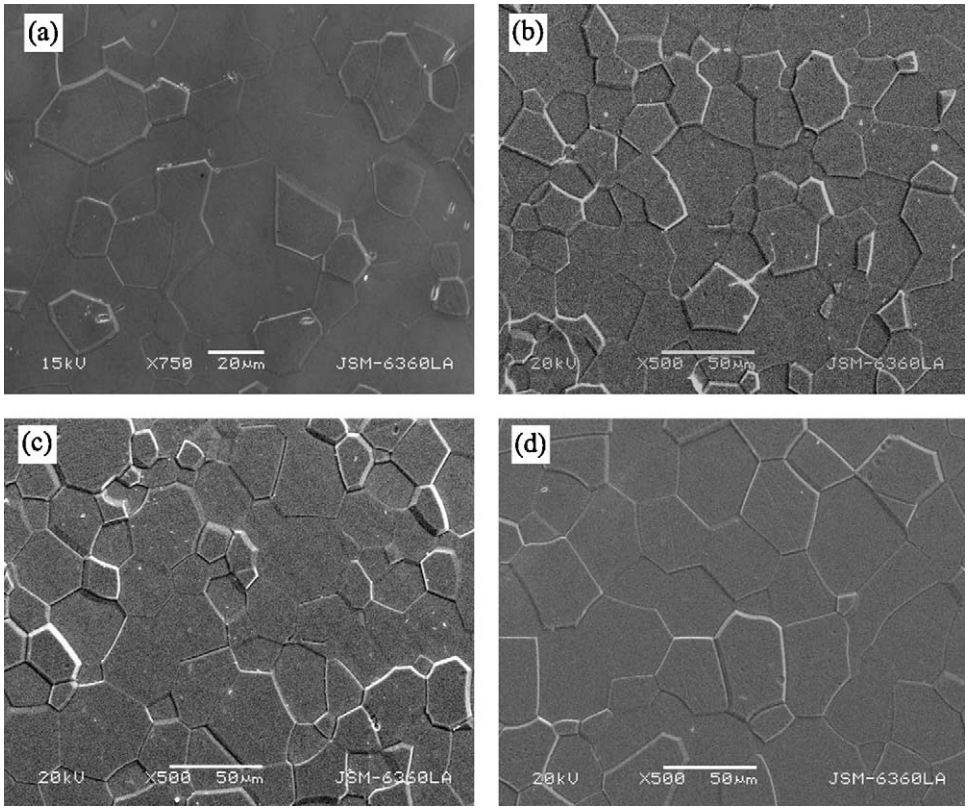

Fig. 2. SEM photographs of Y_2O_3 transparent ceramics with different Yb contents. (a) 0 at.%, (b) 3 at.%, (c) 5 at.% and (d) 8 at.%.

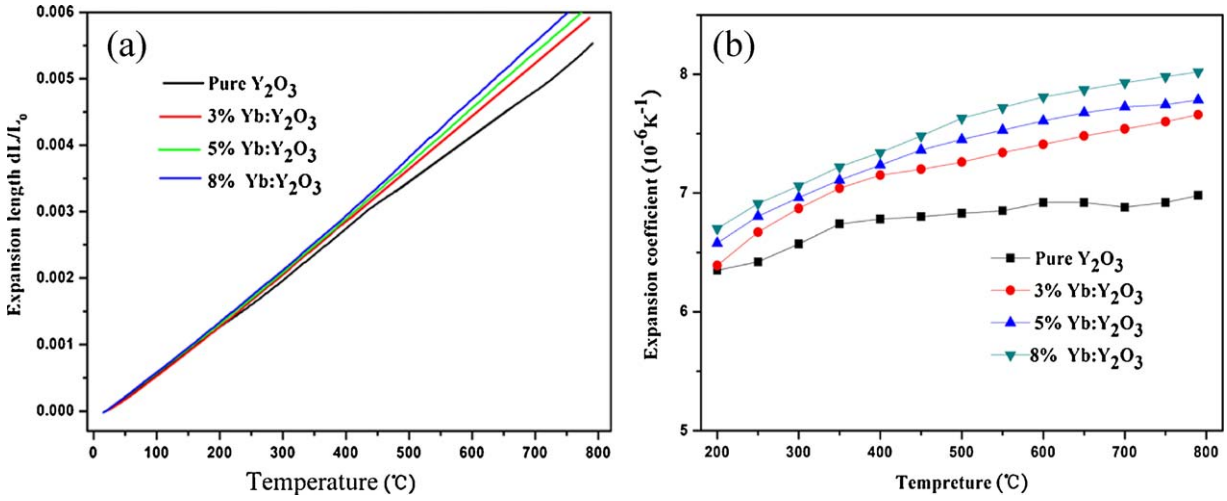

Fig. 3. Thermal expansion (a) and thermal expansion coefficient (b) of Y_2O_3 transparent ceramics with different Yb doping concentrations as a function of temperature.

mal expansion curves are essentially linear in the temperature range from RT to 800 °C, and no anomaly is observed when the measurement is carried out. It is obviously that the thermal expansion length increases with Yb content at the same temperature. Because the ceramic body is isotropic, we can calculate the linear thermal expansion coefficients by the expression below:

$$\alpha = \frac{dL/L_0}{\Delta T} \quad (1)$$

where ΔT is the temperature difference from RT to several other temperatures. Because the dilatometer furnace is not very stable around room temperature especially when it just starts up, the thermal expansion coefficients are not accurate below 200 °C. The coefficients over 200 °C are shown in Fig. 3(b), which clearly shows that the thermal expansion coefficient of Yb:Y_2O_3 transparent ceramic increases with Yb doping concentration. The coefficients from RT to 800 °C are 6.98×10^{-6}, 7.66×10^{-6}, 7.78×10^{-6} and 8.02×10^{-6} K^{-1} for Y_2O_3 transparent ceramic with Yb doping level of 0, 3, 5 and 8%, respectively. This increase is probably due to the structural distortion caused by the doping of Yb^{3+} ions.

The variations in thermal diffusivity and specific heat of Y_2O_3 transparent ceramic as a function of Yb concentration at RT are reported in Fig. 4(a). In this study, we did not take account of the effect of grain size on the heat transfer in Y_2O_3 ceramics due to its small influence.[17] The thermal diffusivity for pure Y_2O_3 transparent ceramic is 5.253×10^{-6} m^2/s, and it reduces as much as 48% to 2.683×10^{-6} m^2/s for 8 at.% Yb:Y_2O_3 transparent ceramic. The reduction of thermal diffusivity is due to the irregularity of ceramic density caused by Yb doping.[18] With Yb concentration increasing, the specific heat of Yb:Y_2O_3 transparent ceramic first decreases and then increases slightly. Because the heavier Yb^{3+} ions (atomic weight: 173.1) substitute for Y^{3+} ions (atomic weight: 88.9), the density of Yb:Y_2O_3 transparent ceramics increases with Yb^{3+} doping content (Fig. 4(b)). The thermal conductivity is calculated using the following equation:

$$k = \alpha \cdot \rho \cdot Cp \quad (2)$$

where k, α, ρ and Cp denote thermal conductivity, thermal diffusion coefficient, density and specific heat, respectively. As displayed in Fig. 4(b), the influence of Yb^{3+} doping concentration on the thermal conductivity is apparent. While the doping content of Yb^{3+} ion increases from 0 to 8 at.%, the thermal conductivity decreases by as much as 46%, from 11.97 to 6.39 W/m/K. Le Garrec and Casagrande predicted the thermal conductivity of 3 at.% Yb:Y_2O_3 ceramic as 6.7 W/m/K by the famous model invented by Gaumé.[18,19] While with 3 at.% ZrO_2 as additive, the thermal conductivity of our prepared 3 at.% Yb:Y_2O_3 ($(Yb_{0.03}Y_{0.94}Zr_{0.03})_2O_3$) is still as high as 7.1 W/m/K. With the development of nano powder fabricating techniques, combined with an optimal preparing process such as slip casting or hot isostatic pressing sintering, the amount of additive (ZrO_2) can be reduced, and the thermal conductivity will increase further, which is advantageous to reduce thermal lensing effects and improve the laser beam quality of Yb:Y_2O_3 ceramic.

The dependence of thermal conductivity of 5 at.% Yb:Y_2O_3 ceramic on temperature is measured and given in Fig. 5. With the temperature increasing, the thermal diffusivity decreases, whereas the specific heat increases, which is in conformity with the numerical model proposed by Sato.[20] Thermal diffusivity describes the ability of thermal equilibrium inside the object. It is difficult to balance the temperature at higher temperature. Therefore, the thermal diffusivity decreases with temperature increasing. Specific heat characterizes the amount of heat required to change a body's temperature by 1 °C, it increases with temperature consequently. The thermal conductivity is 6.46, 5.63, 4.79 and 4.46 W/m/K when the temperature is 25 °C, 100 °C, 200 °C and 300 °C, respectively. It is important to note that, although the thermal conductivity decreases with temperature, it is still higher than that of 5 at.% Yb doped YAG crystal at the same temperature reported in Ref. 21. The heat induced by laser will decrease thermal conductivity, however,

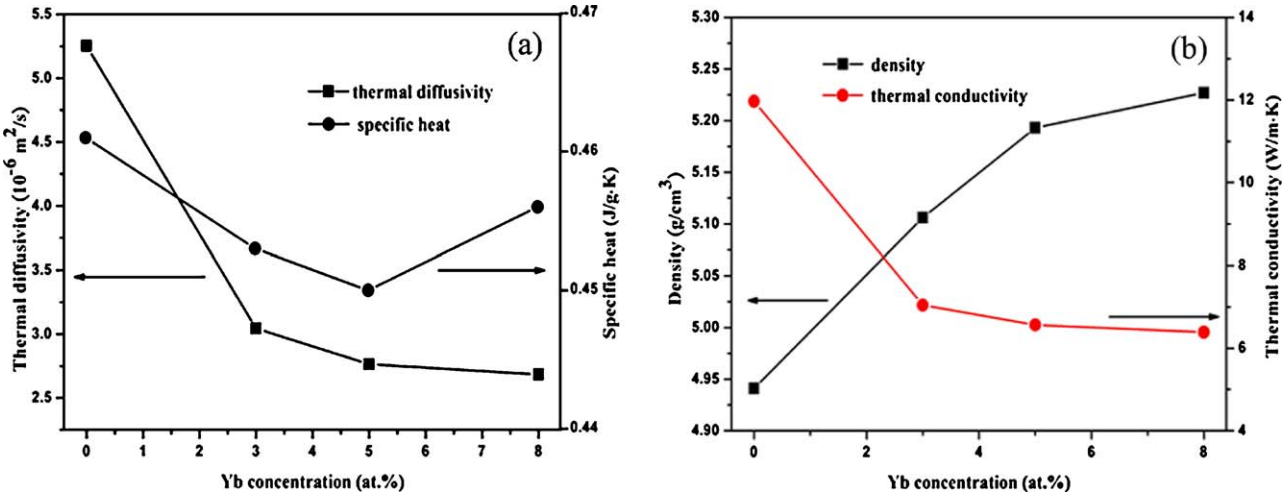

Fig. 4. (a) Thermal diffusivity and specific heat of Y_2O_3 transparent ceramic with different Yb contents. (b) Density and thermal conductivity of Y_2O_3 transparent ceramic with different Yb contents.

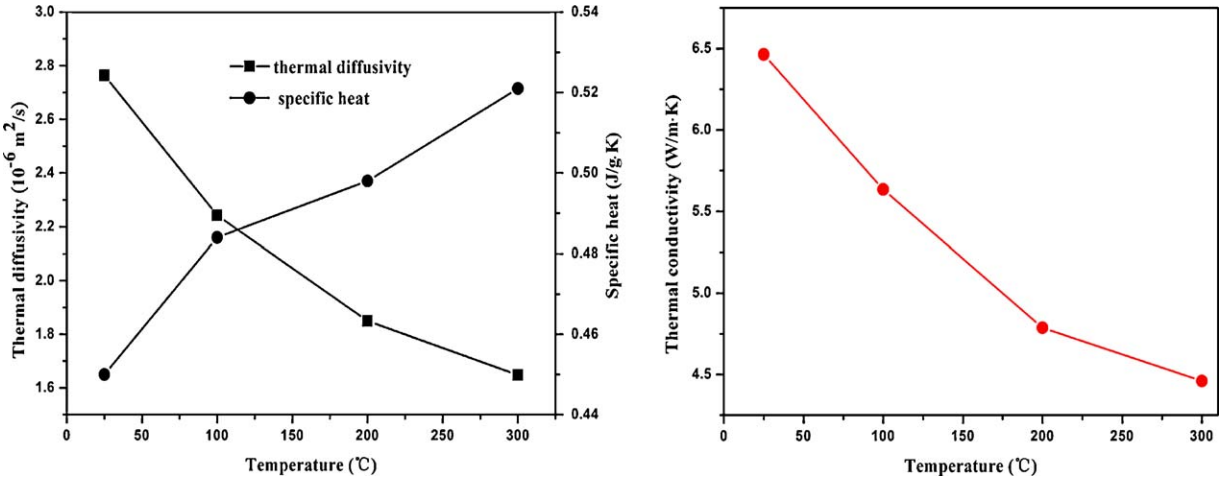

Fig. 5. Thermal diffusivity, specific heat and thermal conductivity of 5 at.% Yb doped Y_2O_3 transparent ceramic as a function of temperature.

the reduction in thermal conductivity will cause heat congregation. This is a vicious cycle which is adverse to the laser quality, so during laser operation, the cooling of Yb:Y_2O_3 transparent ceramic is necessary.[9]

3.3. Mechanical properties

Fig. 6 presents the image of indentation on the mechanically polished surface of Y_2O_3 transparent ceramic. The microhardness can be estimated by the generally accepted formula:

$$H = K\frac{P}{d^2} \tag{3}$$

where P is the load on the indenter; d is the length of indentation diagonal; and K is the shape factor of the indenter, which is equal to 1.854 for a pyramid-shaped indentation. The fracture toughness can be experimentally determined from the linear sizes of radial cracks (C) arising near the point of load application and

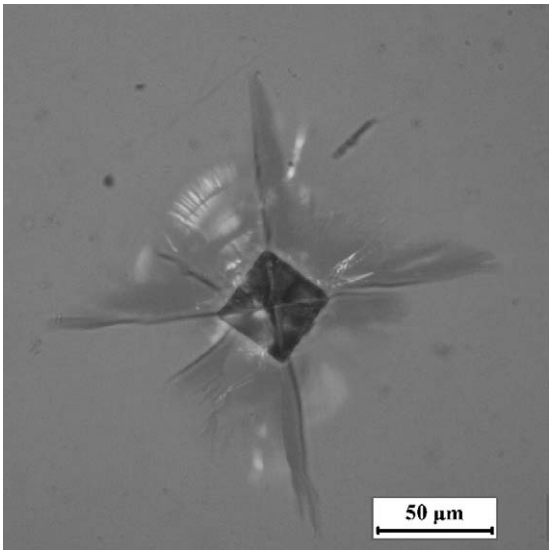

Fig. 6. Microscopic image of indentation in mechanically polished Y_2O_3 ceramic.

estimated by the known formula[22]:

$$K_{IC} = 0.016\left(\frac{E}{H}\right)^{1/2}\left(\frac{P}{C^{3/2}}\right) \quad (4)$$

where E is the Young modulus, which is considered to be 179.8 GPa according to Yeheskel.[23] The calculated microhardness and fracture toughness of Yb:Y_2O_3 ceramics with different Yb concentrations are listed in Table 2. Besides, some reported values are given for comparison.[24,25] It can be seen that our results are in good agreement with the published results and the introduction of substituting Yb ions into Y_2O_3 ceramic somewhat decreases the hardness and K_{IC}. The hardness of Y_2O_3 transparent ceramic not only suits for mechanical processing, such as cutting and polishing, but also has enough mechanical reliability for laser equipment.

4. Conclusion

$(Yb_xY_{0.97-x}Zr_{0.03})_2O_3$ transparent ceramics ($x = 0$, 0.03, 0.05 and 0.08) were fabricated, and the microstructure, thermal and mechanical properties was investigated. With Yb doping concentration increasing from 0 to 8 at.%, the mean grain size increases, whereas the thermal conductivity at RT decreases. The thermal conductivity of 5 at.% Yb:Y_2O_3 transparent ceramic decreases from 6.46 to 4.46 W/m/K when the temperature increases from 25 °C to 300 °C, which is still higher than the reported values of 5 at.% Yb doped YAG crystal at the same temperature. The thermal expansive coefficient and hardness of Y_2O_3 transparent ceramic are appropriate for laser equipment. All the results indicate that Y_2O_3 transparent ceramic is an excellent laser host material.

Acknowledgement

This job is supported by National Natural Science Foundation of China (No. 60676004).

References

1. Hoskins RH, Soffer BH. Stimulated emission from Y_2O_3:Nd^{3+}. *Appl Phys Lett* 1964;**4**:22–3.
2. Brenier, Boulon G. Overview of the best Yb^{3+}-doped laser crystals. *J Alloys Compd* 2001;**323–324**:210–3.
3. Fan TY. Heat generation in Nd:YAG and Yb:YAG. *IEEE J Quantum Electron* 1993;**29**:1457–9.
4. Patel FD, Honea EC, Speth J, Payne SA, Hutcheson R. Laser demonstration of $Yb_3Al_5O_{12}$ (YbAG) and materials properties of highly doped Yb:YAG. *IEEE J Quantum Electron* 2001;**37**:135–44.
5. Brenier A. A new evaluation of Yb^{3+}-doped crystals for laser applications. *J Lumin* 2001;**92**:199–204.
6. Kong J, Tang D, Zhao B, Lu J, Ueda K. 9.2 W diode-end-pumped Yb:Y_2O_3 ceramic laser. *Appl Phys Lett* 2005;**86**:161116.
7. Kong J, Tang DY. Passively Q-switched Yb:Y_2O_3 ceramic laser with a GaAs output coupler. *Opt Express* 2004;**12**:3560–6.
8. Shirakawa A, Takaichi K, Yagi H, Tanisho M, Bisson J-F. First mode-locked ceramic laser: femtosecond Yb^{3+}:Y_2O_3 ceramic laser. *Laser Phys* 2004;**14**:1375–81.
9. Kong J, Tang DY, Chan CC, Lu J, Ueda K, Yagi H, et al. High-efficiency 1040 and 1078 nm laser emission of a Yb:Y_2O_3 ceramic laser with 976 nm diode pumping. *Opt Lett* 2007;**32**:247–9.
10. Zhang HJ, Meng XL, Zhu L, Wang P, Liu XS, Yang ZH. Growth, morphology and characterization of Yb:YVO_4 crystal. *Phys Status Solidi (a)* 1999;**175**:705–10.
11. Peters R, Kränkel C, Petermann K, Huber G. Broadly tunable high-power Yb:Lu_2O_3 thin disk laser with 80% slope efficiency. *Opt Express* 2007;**15**:7075–82.
12. Beil K, Fredrich-Thornton ST, Peters R, Petermann K, Huber G. Yb-doped thin-disk laser materials: a comparison between Yb:LuAG and Yb:YAG. In: *Advanced solid-state photonics, OSA technical digest series (CD) (Optical Society of America, 2009), paper WB28.*; 2009.
13. Li J, Wu Y, Pan Y, Liu W. Fabrication, microstructure and properties of highly transparent Nd:YAG laser ceramics. *Opt Mater* 2008;**31**:6–17.
14. Sato Y, Taira T. Thermal conductivities of polycrystalline Nd^{3+}- and Yb^{3+}-doped $Y_3Al_5O_{12}$ ceramics. In: *Advanced solid-state photonics, OSA technical digest series (CD) (Optical Society of America, 2007), paper WB16.*; 2007.
15. Hou X, Zhou S, Li Y, Li W. *J Eur Ceram Soc* 2010;**30**:3125–9.
16. Hou X, Zhou S, Li Y, Li W. *Opt Mater* 2010;**32**:1435–40.
17. Bission JF, Yagi H, Yanagtani T, Kaminskii A, Barabanenkov YN, Ueda KI. Influence of the grain boundaries on the heat transfer in laser ceramics. *Opt Rev* 2007;**14**:1.
18. Gaumé R, Viana B, Vivien D. A simple model for the prediction of thermal conductivity in pure and doped insulating crystals. *Appl Phys Lett* 2003;**83**:1355–7.
19. Le Garrec B, Casagrande O. Diode pumped Yb doped ceramic laser. In: *3rd international workshop on high energy class diode pumped solid state lasers*. May 2006.
20. Sato Y, Akiyama J, Taira T. Effect of rare-earth doping on the thermal conductivity in $Y_3Al_5O_{12}$ crystals. *Opt Mater* 2009;**31**:720–4.
21. Xu X, Zhao Z, Xu J. Thermal diffusivity, conductivity and expansion of $Yb_{3x}Y_{3(1-x)}Al_5O_{12}$ ($x = 0.05$, 0.1 and 0.25) single crystals. *Solid State Commun* 2004;**130**:529–32.
22. Lawn BR, Evans AG, Marshall DB. Elastic/plastic indentation damage in ceramics: the median/radial crack system. *J Am Ceram Soc* 1980;**63**:574–81.
23. Yeheskel O, Tevet O. Elastic moduli of transparent yttria. *J Am Ceram Soc* 1999;**82**:136–44.
24. Kaminskii AA, Akchurin MSh, Gainutdinov RV, Takaichi K. Microhardness and fracture toughness of Y_2O_3- and $Y_3Al_5O_{12}$-based nanocrystalline laser ceramics. *Crystallogr Rep* 2005;**50**:869–73.
25. Serivalsatit K, Kokuoz B, Kennedy M, Ballato J. Synthesis, processing and properties of submicrometer-grained highly transparent yttria ceramics. *J Am Ceram Soc* 2010;**93**:1320–5.